# Ziv - Zakai Lower Bound on Target Localization Estimation in MIMO Radar Systems

Vlad M. Chiriac, Alexander M. Haimovich

ECE Dept., CWCSPR Lab., New Jersey Institute of Technology, Newark, New Jersey
{vc43, haimovic}@njit.edu

***Abstract*—This paper presents the derivation of the Ziv-Zakai bound (ZZB) for the localization problem in a MIMO radar system. The target is positioned in the near-field of a network of radars of arbitrary geometry. The radars have ideal mutual time and phase synchronization. The target location is estimated by coherent processing exploiting the amplitude and phase information between pairs of radars. An analytical expression is developed for the ZZB relating the estimation mean square error (MSE) to the carrier frequency, signal bandwidth, the number of sensors, and their location. From numerical calculations of the bound, three regions of signal-to-noise ratio (SNR) can be distinguished in the performance of the location estimator: a noise-dominated region, an ambiguity region, and an ambiguity free region. In the noise-dominated region, the signals received by the radars are too weak, and thus the localization error is limited only by the *a priori* information about the location of the target. In the ambiguity region, the performance of the location estimator is affected by sidelobes. In the ambiguity free region, estimation errors are very small and the ZZB approaches the Cramer-Rao lower bound (CRLB).**

***Index Terms*—Target localization, performance bounds, parameter estimation**

## I. Introduction

Localization has been intensively studied and broadly applied in many fields including radar, sonar, seismic analysis, and sensor networks. Due to the many applications, each characterized by its own set of requirements, the localization problem remains an active subject of research. The main figure of merit for the localization problem is accuracy. Recent work on localization of targets in MIMO radar systems has shown the potential for significant gains when localization processing exploits the phase information among pairs of radars [1]. Localization systems that exploit the phase information are referred to as *coherent,* in contrast to *noncoherent* systems, which exploit envelope measurements. Evaluation of the Cramer-Rao lower bound (CRLB) has shown that at high SNR, the accuracy of coherent MIMO radar systems is of the order of the carrier wavelength of the transmitted waveforms [1]. MIMO radar systems with widely distributed elements have high accuracy capabilities of localizing targets, but are also subject to high peak sidelobes in the coherent localization metric [2]. At sufficiently high SNRs, these sidelobes have little impact on performance. Below a threshold SNR however, performance degrades rather quickly. The main goal of this work is to improve the understanding of the effect of sidelobes on MIMO radar performance and develop ways to predict the performance of localization techniques as a function of SNR and of system parameters. The performance of target localization can be studied through a lower bound on the mean square error (MSE) of the localization estimates. For high SNR, the estimated parameter is affected by noise errors that are too small to cast the estimate outside the main lobe of the localization metric. In this region, the mean square error (MSE) of the estimate is inverse proportional to the Fisher information, and thus performance can be predicted by calculating the CRLB, [3]. At low SNR, due to the effect of sidelobes, performance is affected by large errors, and the CRLB cannot predict performance anymore. In this region, performance can be lower bounded by the Ziv-Zakai Bound (ZZB), [4].

In the literature, the ZZB was used as a lower bound for different estimators related to the localization problem. Weiss and Weinstein derived the ZZB for time delay estimation of narrowband [5] and wideband [6] signals. Extending this work, the ZZB for time delay estimation of ultra-wideband signals was studied in [7]. Bell et al. extended the ZZB from scalar to vector parameter estimation [8], and used it to develop a lower bound on the MSE in estimating the 2-D bearing of a narrowband plane wave [9]. The extended ZZB to vector parameter estimation was used for the passive coherent localization problem in [10].

The paper is organized as follows. Section II introduces the system model; the derivation of the ZZB is carried out in Section III. Numerical examples are presented in Section IV, and concluding remarks are found in Section V.

## II. System model

Consider a target located at an unknown position $\boldsymbol{\theta} = [x_e, y_e]$, where $\boldsymbol{\theta}$ is modeled as a continuous random variable with a known *a priori* probability density function (pdf), assumed here to be the uniform distribution $x_e,\ y_e \sim U[-D,\ D]$. This description implies that the target is known to be located somewhere in a square area of dimensions $2D \times 2D$. The target is radiated by $M$ transmitting radars arbitrarily located at coordinates $\mathbf{T}_i = [x_{ti}, y_{ti}]$, $i = 1, \ldots, M$, with a set of orthogonal signals, $s_i$. It is assumed that the orthogonality between different transmitted signals is maintained for all relevant delays. The transmitted signals have bandwidth $B$, and they modulate a carrier frequency $f_c$. The signals scattered by the target are collected by $N$ sensors placed at arbitrary positions $\mathbf{R}_k = [x_{rk}, y_{rk}]$, $k = 1, \ldots, N$. The transmitting radars and the sensors are assumed to be synchronous in time and phase. The period of time $T$ during which the observations are collected is such that $BT \gg 1$. Based on the noisy observations collected, the location of the target is estimated coherently i.e., the location is estimated from amplitude and phase measurements.

The noisy observations of the signals received at the sensors are expressed by:

$$r_k(t) = \sum_{i=1}^{M} a_{i,k} s_i(t - \tau_{i,k}) e^{-j2\pi f_c \tau_{i,k}} + w_k(t) \quad (1)$$

where $s_i$ and $w_k$ denote respectively, the signal transmitted by the $i$-th transmitting radar, and additive noise at the $k$-th sensor. The transmitted signals and the noise waveforms are sample functions of uncorrelated, zero-mean, stationary Gaussian random processes with spectral densities $P_{si}$, $i = 1, \ldots, M$ and $P_w$, respectively. The spectral densities are constant across the bandwidth. The amplitude and the propagation delay of the signal transmitted by the $i$-th transmitting radar and received at $k$-th sensor are denoted $a_{i,k}$ and $\tau_{i,k}$, respectively. It is assumed that the amplitudes $a_{i,k}$ are known or can be estimated based on a priori rough information on the target location. The propagation delay $\tau_{i,k}$ is the sum of the time delays from radar $i$ to the target and from target to sensor $k$. If we denote by $\rho_{ti} = \|\mathbf{T}_i - \boldsymbol{\theta}\|$ the distance between the transmitting radar located at $\mathbf{T}_i$ and the target, and by $\rho_{rk} = \|\mathbf{R}_k - \boldsymbol{\theta}\|$ the distance between the target and the receiving radar located at $\mathbf{R}_k$, $\tau_{i,k}$ can be expressed as:

$$\tau_{i,k} = \frac{1}{c}(\rho_{ti} + \rho_{rk}), \quad (2)$$

where $c$ is the signal propagation speed.

Analysis in the frequency domain is more convenient than in the time domain because in the frequency domain the time delays appear in the argument of the complex exponential function. To make use of properties of the Fourier transform, we convert the time domain measurements to the frequency domain. The $f_l$ Fourier coefficient of the observed signal at sensor $k$ is given by:

$$R_k(f_l) = \frac{1}{\sqrt{T}} \int_0^T r_k(t) e^{-j2\pi f_c t} dt = \\ = \sum_{i=1}^{M} a_{i,k} S_i(f_l) e^{-j2\pi(f_l + f_c)\tau_{i,k}} + W_k(f_l) \quad (3)$$

where $l = 1, \ldots, L$, $L$ is the number of frequency samples, and $S_i(f_l)$ and $W_k(f_l)$ are the Fourier coefficients at $f_l$ of $s_i(t)$ and $w_k(t)$, respectively. For later use, we define the vectors $\mathbf{r} = [\mathbf{r}^T(f_1), \mathbf{r}^T(f_2), \ldots, \mathbf{r}^T(f_L)]^T$, where $\mathbf{r}(f_l) = [R_1(f_l), R_2(f_l), \ldots, R_N(f_l)]^T$. For $BT \gg 1$, any pair of Fourier coefficients is uncorrelated [11]. Since $r_k(t)$ is a Gaussian process and the Fourier transform is a linear operation, $\mathbf{r}$ has a conditional multivariate Gaussian pdf,

$$p(\mathbf{r}|\boldsymbol{\theta}) = \prod_{l=1}^{L} \frac{1}{\det(\pi \mathbf{K}(f_l))} \\ \cdot \exp\left\{-([\mathbf{r}(f_l) - \boldsymbol{\gamma}(f_l)]^H \boldsymbol{K}^{-1}(f_l)([\mathbf{r}(f_l) - \boldsymbol{\gamma}(f_l)]\right\} \quad (4)$$

where

$$\boldsymbol{\gamma}(f_l) = \left[\sum_{i=1}^{M} a_{i,1} S_i(f_l) e^{-j2\pi(f_l+f_c)\tau_{i,1}}, \ldots, \right. \\ \left. \sum_{i=1}^{M} a_{i,N} S_i(f_l) e^{-j2\pi(f_l+f_c)\tau_{i,N}}\right]^T \quad (5)$$

represents the response across the sensors to a radiated frequency component $(f_c + f_l)$, and $\mathbf{K}(f_l) = P_w(f_l)\mathbf{I}$ represents the covariance matrix of the Fourier coefficients at the sensors. The matrix $\mathbf{I}$ is the identity matrix. The superscripts "$T$" and "$H$" denote the transpose and conjugate transpose operations, respectively.

The maximum likelihood estimate of the source location is given by the maximum of the likelihood function

$$\widehat{\boldsymbol{\theta}}_{ML}(\mathbf{r}) = \arg\max_{\boldsymbol{\theta}} p(\mathbf{r}|\boldsymbol{\theta}) \quad (6)$$

where the likelihood function equals the value of the pdf at the observations $\mathbf{r}$. It can be shown that for the model defined in (4), the MLE of $\boldsymbol{\theta}$ is given by the expression:

$$\hat{\boldsymbol{\theta}}_{ML}(\mathbf{r}) = \arg\max_{\boldsymbol{\theta}} \sum_{k=1}^{N} \sum_{i=1}^{M} a_{i,k}^* e^{j2\pi f_c \tau_{i,k}} \cdot \\ \sum_{l=1}^{L} R_k(f_l) S_i^*(f_l) e^{j2\pi f_l \tau_{i,k}} \quad (7)$$

The term $e^{j2\pi f_c \tau_{i,k}}$ which is the phase information reveals the coherent nature of the estimator. It is well known that a linear phased array in which the elements are highly thinned, has a beampattern with large sidelobes. In particular, when the elements of the array are randomly spaced at intervals of the order of 10's or 100's of wavelengths, the beampattern has random peak sidelobes [12]. Recent work on coherent MIMO radar based in a setting of widely spaced transmitters and receivers also shows the presence of large peak sidelobes [2]. This motivates our work to develop a global bound on the localization performance, as presented in the next section.

## III. Localization Estimation Bound

Consider the problem of estimating the position vector, $\boldsymbol{\theta}$, of the emitting source. We are interested in deriving lower bounds for the mean square error (MSE) of the individual components of $\boldsymbol{\theta}$. The lower bounds should predict as nearly as possible the performance of the maximum likelihood estimator (MLE) for the whole SNR region. In the literature, one of the most popular bounds used to predict the performance of the MLE is the Cramer Rao lower bound (CRLB), [3]. The justification of using CRLB resides in that the MLE approaches the CRLB arbitrarily close for very long observations. CRLB is a local bound i.e., it represents the performance of estimators only for small errors. As the SNR decreases, the errors become global and spread beyond the local vicinity of the true value of the estimated parameter. Thus, the CRLB cannot be used to predict the MLE performance under these conditions.

When global errors are of interest, evaluating them is meaningful only if the set of possible values of the parameters to be estimated is known beforehand. This leads to Bayesian type bounds. The characteristic of these bounds is that they assume a random parameter model with known *a priori* distribution. In the literature, several Bayesian bounds were proposed , [13], [4], [14], [15], [16]. In this work, we focus on the Ziv-Zakai bound (ZZB) [4], [14].

Briefly, in its scalar form, the problem is that of lower bounding the MSE

$$E\left[\epsilon^2\right] = E\left[\left|\widehat{\theta}\left(r\right) - \theta\right|^2\right] \tag{8}$$

where $\theta$ is the true value and $\widehat{\theta}$ is the estimate based on the observation $r$. The derivation for the scalar case starts with the MSE computed globally from the identity [8],

$$E\left[\epsilon^2\right] = \frac{1}{2}\int_0^{\infty} \Pr\left(|\epsilon| \geq \frac{h}{2}\right) hdh \tag{9}$$

and focuses on lower bounding $\Pr\left(|\epsilon| \geq \frac{h}{2}\right)$. In other words, the MSE is obtained by averaging all the errors $h$ according to their probabilities $\Pr\left(|\epsilon| \geq \frac{h}{2}\right)$. The lower bound on the MSE is obtained from the lower bound on the error probabilities $\Pr\left(|\epsilon| \geq \frac{h}{2}\right)$. The probability of error $\Pr\left(|\epsilon| \geq \frac{h}{2}\right)$ can be considered from a detection theory point of view by noting that $\Pr\left(|\epsilon| \geq \frac{h}{2}\right)$ is also the probability of a binary hypothesis problem in which $\theta$ equals either some value $\tilde{\theta}_0$ ($H_0$ hypothesis) or the value $\tilde{\theta}_0 + h$ ($H_1$ hypothesis).

In the localization problem, the unknown parameter is represented by a vector $\boldsymbol{\theta}$. Hence, we are interested in the extension of the ZZB to vector parameters. In particular, the extended ZZB for vector parameter estimation, which was derived in [8], is customized in this section for the problem of estimating the position of a target in MIMO radar. For a target with the true location given by the position vector, $\boldsymbol{\theta} = [x_e, y_e]^T$, the error correlation matrix of the estimator $\hat{\boldsymbol{\theta}}(\mathbf{r})$ is

$$\boldsymbol{\Phi} = E_{\boldsymbol{\theta},\mathbf{r}}[\boldsymbol{\epsilon}\boldsymbol{\epsilon}^T] = E_{\boldsymbol{\theta},\mathbf{r}}[(\hat{\boldsymbol{\theta}}(\mathbf{r}) - \boldsymbol{\theta})(\hat{\boldsymbol{\theta}}(\mathbf{r}) - \boldsymbol{\theta})^T], \tag{10}$$

where $\mathbf{r}$ is the observations vector defined previously with conditional pdf given in (4), and $E_{\boldsymbol{\theta},\mathbf{R}}$ is the expectation with respect to the joint pdf of $\boldsymbol{\theta}$ and $\mathbf{r}$. Lower bounding $\mathbf{u}^T\boldsymbol{\Phi}\mathbf{u}$ for any vector $\mathbf{u}$ offers a flexible approach through which the total error (sum of the diagonal elements of $\boldsymbol{\Phi}$) or errors of specific components of $\boldsymbol{\theta}$ can be bounded. For example, for evaluation of the total error, let $\mathbf{u} = [1, 1]^T$; for estimating the error in the $x$ coordinate, $\mathbf{u} = [1, 0]^T$.

An identity similar to (9) can be written for the MSE in vector estimation problems by replacing $|\epsilon|$ with $|\mathbf{u}^T\boldsymbol{\epsilon}|$,

$$\mathbf{u}^T\boldsymbol{\Phi}\mathbf{u} = E\left[|\mathbf{u}^T\epsilon|^2\right] = \frac{1}{2}\int_0^{\infty} \Pr\left(\left|\mathbf{u}^T\epsilon\right| \geq \frac{h}{2}\right) hdh. \tag{11}$$

As discussed previously for the scalar case, the lower bound of $\mathbf{u}^T\boldsymbol{\Phi}\mathbf{u}$ is obtained by linking the estimation of $\boldsymbol{\theta}$ with a binary hypothesis testing problem. The vector parameter $\boldsymbol{\theta}$ is equal to either the vector $\tilde{\boldsymbol{\theta}}_0$ (the true location) or to the vector $\tilde{\boldsymbol{\theta}}_0 + \boldsymbol{\delta}$. The binary decision problem based on a localization estimate $\hat{\boldsymbol{\theta}}(\mathbf{r})$ is formulated as follows:

$$\begin{aligned} \text{Decide } H_0 :& \boldsymbol{\theta} = \tilde{\boldsymbol{\theta}}_0 && \text{if } \mathbf{u}^T\hat{\boldsymbol{\theta}}(r) \leq u^T\tilde{\boldsymbol{\theta}}_0 + \frac{h}{2} \\ H_1 :& \boldsymbol{\theta} = \tilde{\boldsymbol{\theta}}_1 = \tilde{\boldsymbol{\theta}}_0 + \boldsymbol{\delta} && \text{if } \mathbf{u}^T\hat{\boldsymbol{\theta}}(r) \geq u^T\tilde{\boldsymbol{\theta}}_0 + \frac{h}{2} \end{aligned} \tag{12}$$

The probability of error for this detection problem can be lower bounded with the help of the minimum probability of error $P_\epsilon\left(\tilde{\boldsymbol{\theta}}_0, \tilde{\boldsymbol{\theta}}_0 + \boldsymbol{\delta}\right)$ of a binary detection problem, in which the transmitted vectors are either $\tilde{\boldsymbol{\theta}}_0$ or $\tilde{\boldsymbol{\theta}}_1 = \tilde{\boldsymbol{\theta}}_0 + \boldsymbol{\delta}$, $\boldsymbol{\delta}$ is the vector difference between vector $\tilde{\boldsymbol{\theta}}_1$ and vector $\tilde{\boldsymbol{\theta}}_0$. Such a minimum probability of error is associated with the likelihood ratio test for deciding between the two hypotheses.

In [17], it is shown that the extended ZZB for vector parameter estimation in the case of equally likely hypotheses is given by

$$\begin{aligned} \mathbf{u}^T\boldsymbol{\Phi}\mathbf{u} \geq \int_0^{\infty} h \cdot V\Bigg\{ \max_{\boldsymbol{\delta}:\mathbf{u}^T\boldsymbol{\delta}=h} \int_{\boldsymbol{\Theta}} \min[p_{\boldsymbol{\theta}}(\tilde{\boldsymbol{\theta}}_0), p_{\boldsymbol{\theta}}(\tilde{\boldsymbol{\theta}}_0 + \boldsymbol{\delta})] \\ \cdot P_\epsilon(\tilde{\boldsymbol{\theta}}_0, \tilde{\boldsymbol{\theta}}_0 + \boldsymbol{\delta}) d\tilde{\boldsymbol{\theta}}_{\mathbf{0}} \Bigg\} \cdot dh \end{aligned} \tag{13}$$

where $V\{\cdot\}$ is the valley-filling function, and $\boldsymbol{\theta} \in \boldsymbol{\Theta}$, where $\boldsymbol{\Theta}$ is the set of possible values of $\boldsymbol{\theta}$. To get insight into the role of the valley-filling function, one must note that in general, $\Pr\left(\left|\mathbf{u}^T\epsilon\right| \geq \frac{h}{2}\right)$ is a non-increasing function of $h$. Thus, a tighter lower bound of $\Pr\left(\left|\mathbf{u}^T\epsilon\right| \geq \frac{h}{2}\right)$ can be obtained by capping the computed lower bound with a non-increasing function of $h$. This transformation is done by the valley-filling function.

Assuming uniform *a priori* pdf's in the interval $[-D, D]$ for the $x_e$, $y_e$ coordinates of the target, equation (13) can be specialized as follows

$$\begin{aligned} \mathbf{u}^T\boldsymbol{\Phi}\mathbf{u} \geq \int_0^{2D} \frac{h}{4D^2} \cdot \\ \cdot \left\{ \max_{\boldsymbol{\delta}:\mathbf{u}^T\boldsymbol{\delta}=h} \int_{\boldsymbol{\Theta}} P_\epsilon(\tilde{\boldsymbol{\theta}}_0, \tilde{\boldsymbol{\theta}}_0 + \boldsymbol{\delta}) d\tilde{\boldsymbol{\theta}}_{\mathbf{0}} \right\} dh \end{aligned} \tag{14}$$

As can be observed from (14), the main part of the bound is represented by $P_\epsilon(\tilde{\boldsymbol{\theta}}_0, \tilde{\boldsymbol{\theta}}_0 + \boldsymbol{\delta})$. The optimum test for a binary hypothesis problem is known to be the likelihood ratio test, but evaluating the performance of the test does not always result in tractable expressions. When exact calculation of the probability of error is not possible, an asymptotic approximation can be applied instead,[18]. Using this approach, the following approximation for $P_\epsilon(\tilde{\boldsymbol{\theta}}_0, \tilde{\boldsymbol{\theta}}_0 + \boldsymbol{\delta})$ is obtained [3, pp 125]:

$$P_e(\tilde{\boldsymbol{\theta}}_0, \tilde{\boldsymbol{\theta}}_0 + \boldsymbol{\delta}) = \exp\left(\mu(s_m) + \frac{s_m^2}{2}\ddot{\mu}(s_m)\right) Q\left(s_m\sqrt{\ddot{\mu}(s_m)}\right) \tag{15}$$

where $\mu(s)$ is the semi-invariant moment generating function of the likelihood ratio test associated with the binary hypothesis problem between $\tilde{\boldsymbol{\theta}}_0$ and $\tilde{\boldsymbol{\theta}}_0 + \boldsymbol{\delta}$, $\ddot{\mu}(s)$ is the second derivative of $\mu(s)$ with respect to $s$, $s_m$ is the point for which $\dot{\mu}(s_m) = 0$, and $Q(z)$ is the Gaussian integral

$$Q(z) = \int_z^\infty \frac{1}{\sqrt{2\pi}} e^{-v^2/2} dv$$

The semi-invariant moment generating function $\mu(s)$ can be expressed [3, pp 119]

$$\mu(s) = \ln \int p(\mathbf{r}|\tilde{\boldsymbol{\theta}}_0 + \boldsymbol{\delta})^s p(\mathbf{r}|\tilde{\boldsymbol{\theta}}_0)^{1-s} d\mathbf{R} \tag{16}$$

Substituting the expression for $p(\mathbf{r}|\boldsymbol{\theta})$ given in (4) into (16), and using the result from [18, pp 47], the semi-invariant moment generating function can be rewritten as follows

$$\mu(s) = -\frac{s(1-s)}{2} \cdot \cdot \sum_{l=1}^{L} \frac{1}{P_w(f_l)} [\boldsymbol{\gamma}_{\tilde{\boldsymbol{\theta}}_1}(f_l) - \boldsymbol{\gamma}_{\tilde{\boldsymbol{\theta}}_0}(f_l)]^H [\boldsymbol{\gamma}_{\tilde{\boldsymbol{\theta}}_1}(f_l) - \boldsymbol{\gamma}_{\tilde{\boldsymbol{\theta}}_0}(f_l)] \tag{17}$$

where

$$\boldsymbol{\gamma}_{\tilde{\boldsymbol{\theta}}_0}(f_l) = \left[\sum_{i=1}^{M} a_{i,1} S_i(f_l) e^{-j2\pi(f_l+f_c)\tilde{\tau}_{i,1}}, \ldots, \sum_{i=1}^{M} a_{i,N} S_i(f_l) e^{-j2\pi(f_l+f_c)\tilde{\tau}_{i,N}}\right]^T \tag{18}$$

and

$$\boldsymbol{\gamma}_{\tilde{\boldsymbol{\theta}}_1}(f_l) = \left[\sum_{i=1}^{M} a_{i,1} S_i(f_l) e^{-j2\pi(f_l+f_c)(\tilde{\tau}_{i,1}+d_{i,1})}, \ldots, \sum_{i=1}^{M} a_{i,N} S_i(f_l) e^{-j2\pi(f_l+f_c)(\tilde{\tau}_{i,N}+d_{i,N})}\right]^T \tag{19}$$

In these expressions, $d_{i,k}$ represents the difference in propagation delays along the paths $i$-$\tilde{\boldsymbol{\theta}}_1$-$k$ and $i$-$\tilde{\boldsymbol{\theta}}_0$-$k$. The term $d_{i,k}$ is given by:

$$d_{i,k} = \frac{1}{c}(\rho_{ti1} + \rho_{rk1} - \rho_{ti0} - \rho_{rk0})$$

where $\rho_{ti1} = \left\|\mathbf{T}_i - \tilde{\boldsymbol{\theta}}_1\right\|$, $\rho_{rk1} = \left\|\mathbf{R}_k - \tilde{\boldsymbol{\theta}}_1\right\|$, $\rho_{ti0} = \left\|\mathbf{T}_i - \tilde{\boldsymbol{\theta}}_0\right\|$, and $\rho_{rk} = \left\|\mathbf{R}_k - \tilde{\boldsymbol{\theta}}_0\right\|$. Since $\tilde{\boldsymbol{\theta}}_0$ represents the true target location and $\tilde{\boldsymbol{\theta}}_1$ represents an erroneous target location, it follows that $d_{i,k}$ are time delay terms associated with erroneous target locations.

Differentiating equation (17) with respect to $s$ yields:

$$\dot{\mu}(s) = -\frac{1-2s}{2} \cdot \sum_{l=1}^{L} \frac{1}{P_w(f_l)} [\boldsymbol{\gamma}_{\tilde{\boldsymbol{\theta}}_1}(f_l) - \boldsymbol{\gamma}_{\tilde{\boldsymbol{\theta}}_0}(f_l)]^H [\boldsymbol{\gamma}_{\tilde{\boldsymbol{\theta}}_1}(f_l) - \boldsymbol{\gamma}_{\tilde{\boldsymbol{\theta}}_0}(f_l)] \tag{20}$$

Differentiating once again,

$$\ddot{\mu}(s) = \sum_{l=1}^{L} \frac{1}{P_w(f_l)} [\boldsymbol{\gamma}_{\tilde{\boldsymbol{\theta}}_1}(f_l) - \boldsymbol{\gamma}_{\tilde{\boldsymbol{\theta}}_0}(f_l)]^H [\boldsymbol{\gamma}_{\tilde{\boldsymbol{\theta}}_1}(f_l) - \boldsymbol{\gamma}_{\tilde{\boldsymbol{\theta}}_0}(f_l)] \tag{21}$$

Solving $\dot{\mu}(s_m) = 0$, yields $s_m = \frac{1}{2}$. Substituting $\mu(s_m)$, $\ddot{\mu}(s_m)$ and $s_m = \frac{1}{2}$ into (15), results in:

$$P_e(\tilde{\boldsymbol{\theta}}_0, \tilde{\boldsymbol{\theta}}_0 + \boldsymbol{\delta}) = Q\left(\frac{1}{2}\sqrt{\ddot{\mu}\left(\frac{1}{2}\right)}\right) \tag{22}$$

Using the fact that the transmitted signals are orthogonal to each other, and $BT \gg 1$, $\ddot{\mu}(s_m)$ is:

$$\ddot{\mu}\left(\frac{1}{2}\right) = 2BT \sum_{k=1}^{N} \sum_{i=1}^{M} a_{i,k}^2 \frac{P_{si}}{P_w} \left[1 - \frac{\sin(\pi B d_{i,k})}{\pi B d_{i,k}} \cos(2\pi f_c d_{i,k})\right] \tag{23}$$

The final version of the ZZB lower bound for the location estimate is:

$$\mathbf{u}^T \Phi \mathbf{u} = \frac{1}{4D^2} \cdot \int_0^{2D} h \left\{ \max_{\boldsymbol{\delta}:\mathbf{u}^T\boldsymbol{\delta}=h} (2D - u_1\delta_1)(2D - u_2\delta_2) Q\left(\frac{1}{2}\sqrt{\ddot{\mu}\left(\frac{1}{2}\right)}\right)\right\} dh \tag{24}$$

Note that $\ddot{\mu}\left(\frac{1}{2}\right)$ in (23) depends on the distance $h$ between hypotheses through the terms $d_{i,k}$. Further insight can be gained by observing that the ZZB decreases with the probability of error $P_e(\tilde{\boldsymbol{\theta}}_0, \tilde{\boldsymbol{\theta}}_0 + \boldsymbol{\delta})$ (see (14)) and that $P_e(\tilde{\boldsymbol{\theta}}_0, \tilde{\boldsymbol{\theta}}_0 + \boldsymbol{\delta})$ is monotonically decreasing with the argument of the Gaussian integral, i.e., with $\ddot{\mu}\left(\frac{1}{2}\right)$. A closer inspection of $\ddot{\mu}\left(\frac{1}{2}\right)$ in ((23)) is then warranted. For a transmitter-receiver pair $i$-$k$, the factor $2BTa_{i,k}^2\frac{P_{si}}{P_w}$ serves as an SNR term. Not surprisingly, increasing the SNR, reduces the MSE of localization. More interesting is the factor $\psi(\boldsymbol{\delta})$,

$$\psi(\boldsymbol{\delta}) = \sum_{k=1}^{N} \sum_{i=1}^{M} \frac{\sin(\pi B d_{i,k})}{\pi B d_{i,k}} \cos(2\pi f_c d_{i,k}) \tag{25}$$

This factor has peaks at time delays $d_{i,k}$ that are multiples of $1/f_c$. Each peak represents a location associated with an increased probability of error. Thus peaks of $\psi(\boldsymbol{\delta})$ correspond to ambiguities marked by peaks sidelobes in the localization metric (7). Increasing the carrier frequency increases the

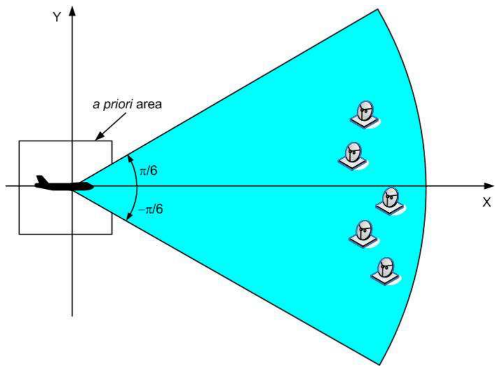


Figure 1. Setup configuration of the MIMO radar system with antennas distributed in a sector.

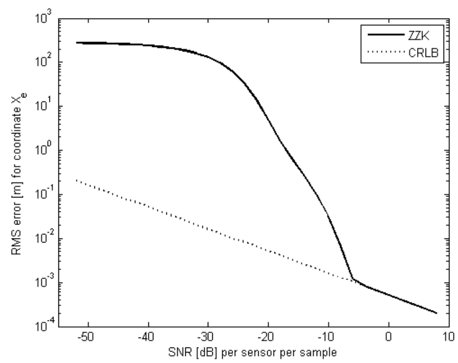


Figure 2. MIMO $2 \times 4$ antennas, $B = 200$ kHz, $f_c = 1$ GHz, and coordinates $x_e$ and $y_e$ uniformly distributed in $[-500$ m, $500$ m$]$ with variance $\sigma^2_{x_e} = \frac{500^2}{3}$ .

density of ambiguities over an area, and indirectly the MSE for SNR regions where the ambiguities dominate. The term $\frac{\sin(\pi B d_{i,k})}{\pi B d_{i,k}}$ corresponds to the autocorrelation of a transmitted pulse (assumed rectangular). This term caps the effect of ambiguities, particularly away from the mainlobe of the localization metric. The effect of ambiguities is reduced by increasing the bandwidth $B$ of the transmitted signals. This observation is consistent with [19]. Ambiguity sidelobes affect the ZZB when they are large enough to compete with the mainlobe of the localization metric. Increasing the number of transmitting stations $M$ and receiving stations $N$, reduces the effect of ambiguities relative to the mainlobe. To explain that, we note that each transmitter-receiver pair has its own pattern of ambiguities. Ambiguities impact performance when ambiguities from multiple transmitter-receiver pairs happen to build up at a specific location. Increasing the number of radars leads to a stronger mainlobe and requires that a larger number of sidelobes build up to compete with the mainlobe. Since the sidelobe build up from multiple transmitter-receiver pairs is a random event, the chances of a large number of sidelobes lining up at one location are small. Thus performance improves with an increase in the number of radars.

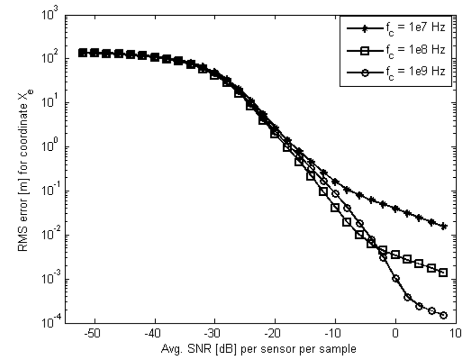


Figure 3. MIMO $2 \times 4$ antennas, $B = 200$ kHz, and coordinates $x_e$ and $y_e$ uniformly distributed in $[-500$ m, $500$ m$]$

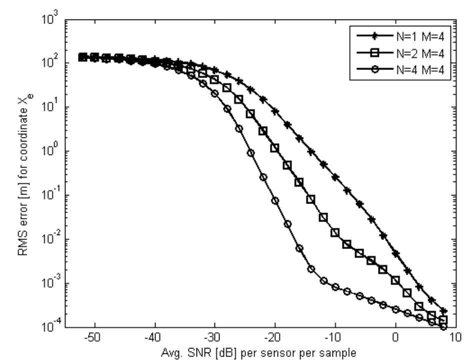


Figure 4. $B = 200$ kHz, $f_c = 1$ GHz, and coordinates $x_e$ and $y_e$ are uniformly distributed in $[-500$ m, $500$ m$]$

## IV. Numerical Results

In this section, numerical examples are provided to illustrate the ZZB for various cases of the target localization problem. We present results of the ZZB parameterized by the carrier frequency, bandwidth, and number of transmit and receive antennas in the system.

The numerical results were obtained for a setup in which the target was positioned in the center of the coordinate system. The transmitting and receiving radars were distributed randomly in a sector with center at the origin of the axes $(0, 0)$ and with a central angle of $\pi/3$ radians. The ZZB was computed numerically by averaging over 30 random setups (different radar configurations). The setup is shown in Fig. 1. The duration of the observation $T$ was taken such that $BT = 625$ samples, where $B$ is the bandwidth in Hz.

In Fig. 2, the ZZB obtained by numerical integration of (24) is plotted versus the average SNR, SNR$= E\left[a^2_{i,k}\frac{P_{si}}{P_w}\right]$ ( $E[]$ means expectation with respect to the random amplitudes $a_{i,k}$) for a $2 \times 4$ MIMO configuration (2 transmit and 4 receive antennas) and transmitted signals with bandwidth $B = 200$ kHz and carrier $f_c = 1$ GHz. The CRLB of the target location is also plotted for reference. The *a priori* interval for the coordinates of the source is set to a square with a side equal to 1 km. From the figure it can be observed that the ZZB versus

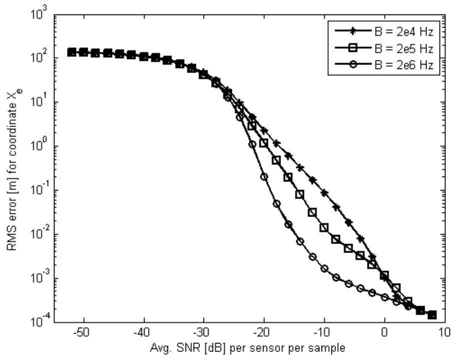


Figure 5. MIMO $2 \times 4$ antennas, $f_c = 1$ GHz, and coordinates $x_e$ and $y_e$ uniformly distributed in $[-500 \text{ m}, 500 \text{ m}]$

SNR can be divided into three regions. For low SNR, the ZZB reaches a plateau equal to the standard deviation of the *a priori* pdf of the source location, computed as $\sqrt{\frac{D^2}{3}} = \frac{500}{\sqrt{3}}$. In this region performance is dominated by noise, hence the localization error is limited only by the *a priori* information. For high SNR, the ZZB merges with the CRLB, indicating that the noise errors are too small to cast the estimate outside the mainlobe of the localization metric. This region is the ambiguity free region. Between the two SNR extremes, is the ambiguity region, in which the location estimator is affected by ambiguities created by sidelobes of the localization metric, [2].

In Fig. 3, the ZZB of the error in estimating the abscissa $x_e$ of the source is presented for different carrier frequencies. The results presented in the figure were obtained for a $2 \times 4$ MIMO system and $B = 200$ kHz signal bandwidth. The *a priori* interval for the abscissa $x_e$ of the narrowband source was set to [-500 m, 500 m] around the real abscissa. One can observe that if the SNR is high enough, localization accuracy improves with the carrier frequency. As predicted by the discussion in the preceding section, in the ambiguity region, the performance degrades with increasing carrier frequency. This result is explained by the increase in sidelobes with the carrier frequency. The effect of sidelobes in the localization metric can be reduced by increasing the number of sensors. This is illustrated in Fig. 4. The effect of bandwidth on localization is shown in Fig. 5. An increase in bandwidth leads to a reduction in the sidelobes, leading to smaller errors in the ambiguity region. This is due to the fact that the transmitted pulse autocorrelation function serves as the envelope of the localization metric. This envelope, which becomes narrower with the increase in bandwidth, forces the sidelobes to decay faster.

## V. CONCLUSIONS

The Ziv-Zakai bound for vector parameters was used to derive a lower bound on the MSE of estimating the location of a target with a MIMO radar system. The bound is a convenient tool for analyzing the localization performance for different parameters such as carrier frequency, signal bandwidth, and number of sensors. From the shape of the bound plotted versus SNR, three SNR regions are distinguishable. At low SNR, performance is dominated by noise, with false peaks popping up anywhere in the a priori parameter space of the source location. As the SNR increases, a transition region is observed, in which performance is dominated by the peak sidelobes of the localization metric. The performance at high SNR is ambiguity free, and the ZZB coincides with the CRLB.

## REFERENCES


[1] N. Lehmann, A. Haimovich, R. Blum, and L. Cimini, "High resolution capabilities of MIMO radar," *40th Asilomar Conf. Signals, Systems and Computers*, pp. 25–30, Oct. 2006.

[2] M. Haleem and A. Haimovich, "On the distribution of ambiguity levels in MIMO radar," *Asilomar Conf. Signals, Systems and Computers*, Oct. 2008.

[3] H. L. V. Trees, *Detection, Estimation, and Modulation Theory, Part I*. New York: Wiley, 2001.

[4] J. Ziv and M. Zakai, "Some lower bounds on signal parameter estimation," *IEEE Trans. Inf. Theory*, vol. 15, pp. 386–391, May 1969.

[5] A. Weiss and E. Weinstein, "Fundamental limitations in passive time delay estimation - Part I: Narrow-band systems," *IEEE Trans. Acoust., Speech, Signal Process.*, vol. 31, pp. 472–486, Feb. 1983.

[6] ——, "Fundamental limitations in passive time delay estimation - Part II: Wide-band systems," *IEEE Trans. Acoust., Speech, Signal Process.*, vol. 32, pp. 1064–1078, Oct. 1984.

[7] B. M. Sadler, L. Huang, and Z. Xu, "Ziv-Zakai time delay estimation bound for ultra-wideband signals," *IEEE International Conference on Acoustics, Speech, and Signal Processing*, vol. 3, pp. 549–552, Apr. 2007.

[8] K. L. Bell, Y. Steinberg, Y. Ephraim, and H. L. V. Trees, "Extended Ziv-Zakai lower bound for vector parameter estimation," *IEEE Trans. Inf. Theory*, vol. 43, pp. 624–637, Mar. 1997.

[9] K. L. Bell, Y. Ephraim, and H. L. V. Trees, "Explicit Ziv-Zakai lower bound for bearing estimation," *IEEE Trans. Signal Process.*, vol. 44, pp. 2810–2824, Nov. 1996.

[10] V. M. Chiriac, A. M. Haimovich, S. C. Schwartz, and J. A. Dabin, "Performance bound for localization of a near field source," *43ed Asilomar Conf. Signals, Systems and Computers*, Nov. 2009.

[11] A. Papoulis, *Probability Random Variables and Stochastic Processes*. McGraw Hill, 1991.

[12] B. D. Steinberg, "The peak sidelobe of the phased array having randomly located elements," *IEEE Trans. on Antennas and Propagation*, vol. AP-20, pp. 129–136, March 1972.

[13] E. W. Barankin, "Locally best unbiased estimates," *Ann. Math. Stat.*, vol. 20, pp. 477–501, 1949.

[14] D. Chazan, M. Zakai, and J. Ziv, "Improved lower bounds on signal parameter estimation," *IEEE Trans. Inf. Theory*, vol. 21, pp. 90–93, Jan. 1975.

[15] A. J. Weiss, "Fundamental bounds in parameter estimation," Ph.D. dissertation, Tel-Aviv University, Tel-Aviv, Israel, 1985.

[16] E. Weinstein and A. J. Weiss, "A general class of lower bounds in parameter estimation," *IEEE Trans. Inf. Theory*, vol. 34, pp. 338–342, Mar. 1988.

[17] S. Bellini and G. Tartara, "Bounds on error in signal parameter estimation," *IEEE Trans. Commun.*, vol. 22, pp. 340–342, Mar. 1974.

[18] L. D. Collins, "Asymptotic approximation to the error probability for detecting Gaussian signals," Ph.D. dissertation, Massachusetts Institute of Technology, Cambridge, MA, 1968.

[19] M. Haleem and A. Haimovich, "Sidelobe mitigation in MIMO radar with multiple subcarriers," *IEEE Radar Conference*, May 2009.